11ª Coteq 2011 Porto de Galinhas PERNAMBUCO
Conferência sobre Tecnologia de Equipamentos
10 a 13 de maio de 2011

COTEQ-149

AN IMPROVED MULTIAXIAL RAINFLOW ALGORITHM

Marco Antonio Meggiolaro[1]
Jaime Tupiassú Pinho de Castro[1]

SYNOPSIS

Non-proportional (NP) multiaxial fatigue life predictions require the use of a multiaxial rainflow algorithm together with a method to calculate the effective stress or strain ranges associated with each counted cycle [1]. The objective of this work is to develop a simple multiaxial rainflow algorithm that allows the proper calculation of multiaxial damage in non-periodic NP histories and to periodic NP histories formed by complex blocks with multiple cycles each. It is shown that Wang-Brown's (WB) multiaxial rainflow algorithm [2] has a few idiosyncrasies that can lead to non-conservative predictions, incorrectly filtering out significant events within a multiaxial loading cycle. An improved multiaxial rainflow algorithm is proposed, called Modified Wang Brown (MWB). It has two main improvements over the WB algorithm. First, the criterion to choose the point where the count is started is modified. Examples are shown to prove that the original criterion can overlook the most damaging event from the history, as opposed to the modified version. And second, the algorithm implementation is significantly simplified when formulated in the reduced five-dimensional Euclidean space defined in [3]. Under plane stress conditions, the algorithm is further simplified using a three-dimensional Euclidean space based on the deviatoric stresses or strains. A simple pseudo-code is presented to efficiently implement the multiaxial count, allowing a fast and efficient calculation of fatigue damage even for very long non-periodic NP histories.

---

1 Mechanical Engineer, PhD, Mechanical Engineering Department, PUC-Rio, Brasil

1. INTRODUCTION

Traditional fatigue life prediction methods under variable amplitude non-proportional (VA-NP) loadings are usually applicable only to periodic histories or to infinite life calculations. Finite life calculations can be performed, but usually the available models implicitly assume that each block of the periodic loading path contains a single cycle. To generalize the existing methods to finite life predictions in periodic histories with multiple cycles at each block or period, or to non-periodic histories, a cycle counting algorithm must be introduced.

The rainflow algorithm [4-5] is reputably the best approach to identify the most damaging events embedded in a variable amplitude history. For linear elastic uniaxial histories, it is indifferent to perform the uniaxial rainflow count on the stresses or on the strains. In addition, the sequential rainflow count is always a better option over the traditional rainflow, since it preserves the original loading order. The sequential rainflow [6-7] is obtained by simply reordering the resulting traditional rainflow count by the final counting point. Even for linear elastic problems, where the damage caused by each event should not depend on the other events nor on the loading order, it is a good idea to choose the sequential rainflow to correctly predict in which event the accumulated damage reaches its critical value (usually 1.0, according to Miner [8]). It is also recommended for crack growth predictions, to correctly account for load interaction effects without changing the load order.

For elastoplastic uniaxial histories, it is fundamental to calculate the hysteresis loops before performing any rainflow count. After measuring/calculating both stress and strain histories, the sequential rainflow count must be applied to the strains, never to the stresses. For multiaxial problems, however, the uniaxial rainflow of stresses or strains may lead to significant errors, even in the linear elastic case, as discussed in the next section.

2. RAINFLOW OF A MULTIAXIAL HISTORY

For general NP multiaxial histories, the traditional unixial rainflow count, applied to some stress or strain component that is assumed dominant to describe the history, does not provide good life predictions. This is so because the peaks and valleys of the stresses and the corresponding strains do not usually coincide, even in the same direction, not to mention in different directions.

Another important issue involves the common practice of filtering non-reversals from a measured history. When dealing with measured multiaxial loading histories, the sampling points that do not constitute a reversal in any of its stress or strain components are usually eliminated. Filtering points that do not constitute a reversal helps to decrease computational cost in multiaxial fatigue calculations, especially when dealing with over-sampled data [9].

But filtering out all points that do not constitute a reversal in one stress or strain component may cause significant damage prediction problems, discussed next. First, the reversal points obtained from a multiaxial rainflow algorithm may not occur at the reversal of one of the stress or strain components. E.g., the relative Mises strain, used in Wang-Brown's rainflow count [1], may reach a peak value at a point that is not a maximum or minimum of any strain component. But this most important point would have been filtered by any non-reversal filtering algorithm, compromising the results.

The second problem may occur because the entire path between two reversals is needed to evaluate the equivalent stress or strain associated with each count. Filtering out points along such path would almost certainly result in lower equivalent stress or strain estimates than expected.

Another issue with rainflow counting NP multiaxial histories is whether or not to use a critical plane approach. The Wang-Brown multiaxial rainflow algorithm is general enough to be directly applied to a multiaxial history involving all 6 strain components [1]. But the counted cycles will probably occur in different planes, not reproducing the crack initiation mechanism.

Instead, a critical plane approach must be followed: the multiaxial history must be projected onto a candidate plane, and only then should a multiaxial rainflow count be used. In this critical plane approach, the stress and/or strain history is projected onto a candidate plane from the critical point. A uniaxial rainflow count is then applied to an appropriate strain or stress component, which depends on the chosen damage model: for the εN and Smith-Wastson-Topper (SWT) [1] damage models, the normal strain perpendicular to the candidate plane is rainflow counted; in the Brown-Miller, Fatemi-Socie and Wang-Brown damage models [1], a shear strain component acting parallel to the candidate plane is rainflow counted; and in the Findley damage model [1], a shear stress component parallel to the candidate plane is counted.

While performing such rainflow count on the candidate plane, the other stress and strain components cannot be overlooked or discarded. For instance, if the SWT damage model is used, at every rainflow counted half cycle ε_I, the maximum value of the normal stress $\sigma_{\perp I}$ parallel to ε_I along the entire half cycle must be stored to compute $\sigma_{\perp Imax}$. Since for complex NP multiaxial load histories these maxima may happen at any point along the half cycle, not only at the peaks and valleys of a given component, non-reversals should never be filtered before performing the rainflow count.

Note also that, if only the strain (or stress) history is provided, one might need to calculate the entire stress-strain history from proportional multiaxial stress-strain relations or from incremental plasticity techniques, before performing the rainflow count. After performing the rainflow count at each candidate plane, the resulting damage is calculated. The critical plane is then the candidate plane that results in the highest fatigue damage.

However, it must be noted that Case B cracks (defined in [1]) can have two shear strain (or stress) components acting parallel to each candidate plane. A uniaxial rainflow approach would either neglect the effect of one of such shear components, or consider that one of them is dominant over the other during the rainflow algorithm application. But this practice can be ***non***-conservative, since both shear components induce crack initiation. To deal with that, a true multiaxial rainflow algorithm must be used, accounting for all stress or strain components, such as Wang-Brown's algorithm, discussed next.

3. WANG-BROWN'S MULTIAXIAL RAINFLOW ALGORITHM

Wang and Brown [10] proposed an interesting multiaxial generalization of the rainflow count that is applicable to any proportional or NP history of strains (or stresses, with simple modifications to the algorithm). Wang-Brown's multiaxial rainflow is based on the Mises strain ε_{Mises} as an indirect measure of fatigue damage.

The problem with using ε_{Mises} is the loss of the loading event sign, since Mises values are always positive. Therefore, in 90° out-of-phase histories it is even possible that ε_{Mises} remain constant, which would wrongfully result in an infinite life prediction. To solve this issue, the relative Mises strain ε_{RMises} is used, calculated from the difference between the strain components $(\varepsilon_{xj}, \varepsilon_{yj}, \varepsilon_{zj}, \gamma_{xyj}, \gamma_{xzj}, \gamma_{yzj})$ of each (j^{th}) point in the history and the strain components $(\varepsilon_{xi}, \varepsilon_{yi}, \varepsilon_{zi}, \gamma_{xyi}, \gamma_{xzi}, \gamma_{yzi})$ of the initial (i^{th}) point of the current count:

$$\varepsilon_{RMises} = \frac{\sqrt{(\Delta\varepsilon_x - \Delta\varepsilon_y)^2 + (\Delta\varepsilon_x - \Delta\varepsilon_z)^2 + (\Delta\varepsilon_y - \Delta\varepsilon_z)^2 + 1.5(\Delta\gamma_{xy}^2 + \Delta\gamma_{xz}^2 + \Delta\gamma_{yz}^2)}}{\sqrt{2}\cdot(1+\bar{\nu})} \tag{1}$$

where $\Delta\varepsilon_x \equiv \varepsilon_{xj} - \varepsilon_{xi}$, $\Delta\varepsilon_y \equiv \varepsilon_{yj} - \varepsilon_{yi}$, $\varepsilon_z \equiv \varepsilon_{zj} - \varepsilon_{zi}$, $\Delta\gamma_{xy} \equiv \gamma_{xyj} - \gamma_{xyi}$, $\Delta\gamma_{xz} \equiv \gamma_{xzj} - \gamma_{xzi}$, $\Delta\gamma_{yz} \equiv \gamma_{yzj} - \gamma_{yzi}$, and $j > i$.

The relative strains need to be re-calculated for every initial counting point, a computationally intensive task for very long histories. Note however that the relative strain ε_{RMises} is only used to locate the initial and final counting points of each half cycle, after which it is possible to apply at these points any multiaxial damage model (even models that do not include a Mises strain parameter).

As in the uniaxial case, Wang-Brown's multiaxial rainflow is based on 3 simple rules:

1. The first count must start at the point with the largest value of ε_{Mises} from the entire history.
2. Each count must be initiated sequentially at each peak or valley of a strain component, and the relative Mises strain ε_{RMises} of the subsequent history must be computed with respect to the initial point.
3. The final point of each count is obtained when reaching:
   a) the largest value of ε_{RMises} with respect to the initial point of the history, or
   b) any path used in a previous count.

Note that the maxima and minima of each stress or strain component may not happen at the beginning or at the end of the counted half cycle, as discussed before. It may happen at any point along the cycle. Therefore, any stress or strain range must be computed considering the maximum and minimum values along the entire path between two reversions, not only the initial and final values from the half cycle.

The following example clarifies the necessary steps to implement this routine. The objective is to rainflow count the multiaxial NP history of cyclic tension-torsion formed by successive blocks of normal and shear strains given by $(\varepsilon_x, \gamma_{xy}) = \{(2, 1) \rightarrow (-1, 2) \rightarrow (2, -2) \rightarrow (-2, -2) \rightarrow (2, 2) \rightarrow (-2, 0)\}\%$ repeatedly applied to a steel specimen, see Fig. 1.

Assuming the elastic Poisson coefficient $\nu_{el} = 0.3$ and $\varepsilon_{el} \cong \varepsilon_{pl}$, the effective Poisson coefficient [1] is

$$\bar{\nu} = \left(\nu_{el}\varepsilon_{el} + 0.5\varepsilon_{pl}\right) / \left(\varepsilon_{el} + \varepsilon_{pl}\right) = 0.4 \tag{2}$$

Defining $\varepsilon \equiv \varepsilon_x$ and $\gamma \equiv \gamma_{xy}$, and using Hooke's law assuming $\sigma_y = \sigma_z = 0$, one can obtain

$$\varepsilon_y = \varepsilon_z = -\bar{\nu}\varepsilon \Rightarrow \varepsilon_{Mises} = \sqrt{\varepsilon^2 + 3[\gamma/(2+2\bar{\nu})]^2} \tag{3}$$

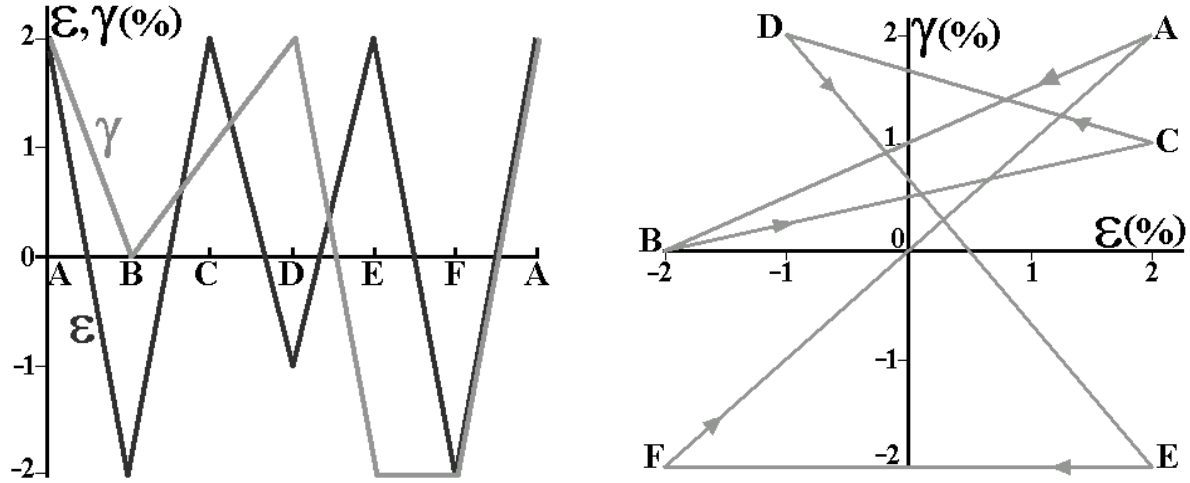

Fig. 1: Strain history for the considered NP loading and corresponding γ-ε diagram.

Translating the block to begin at the point with highest absolute ε_{Mises} (point $A = (2, 2)$, even though points E and F have the same ε_{Mises} in the time history shown in Fig. 1), the γ-ε diagram from Fig. 1 is obtained. The initial point of the first event of the rainflow count is $A(2, 2)$. The relative Mises strains with respect to A are given by

$$\varepsilon_{R_{Mises}}(A) = \sqrt{(\varepsilon - 2\%)^2 + 3 \cdot [(\gamma - 2\%)/(2 + 2\bar{\nu})]^2} \tag{4}$$

resulting in the relative history from Fig. 2. The count of this first event stops at point F, which has the highest ε_{RMises} with respect to A, see Fig. 2. Note that in the path B-B' of Fig. 2 the value of ε_{RMises} is constant, therefore in the corresponding γ-ε diagram it describes an arc of ellipse centered in A. Along the entire path A-B-B'-F, the highest value of $\varepsilon = 2\%$ takes place at point A, and the lowest $\varepsilon = -2\%$ takes place at B and F. The highest $\gamma = 2\%$ also takes place at A, and the lowest $\gamma = -2\%$ takes place at the entire path B'-F. In this way, according to Wang-Brown's method, in this half cycle we obtain the absolute ranges $\Delta\varepsilon = 4\%$ and $\Delta\gamma = 4\%$.

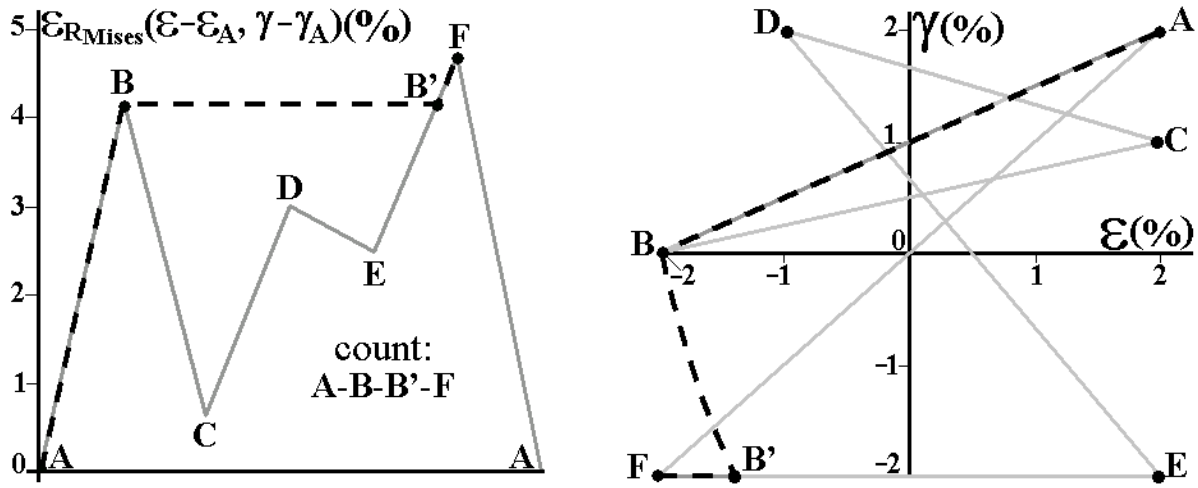

Fig. 2: Rainflow count of the 1st event of the history and corresponding γ-ε diagram.

Note that the calculation of the exact location of point *B'* in the path *E-F* of the γ-ε diagram is important to obtain the ranges $\Delta\varepsilon$ and $\Delta\gamma$ from the following counts. The position is obtained finding the interpolation parameter α from $B' = (\varepsilon, \gamma) = (2, -2) + \alpha \cdot [(-2, -2) - (2, -2)]$ that makes the ε_{RMises} of *B'* with respect to *A* equal to *4.19%* (which is equal to the ε_{RMises} of point *B* with respect to *A*), hence

$$\varepsilon_{R_{Mises}}(A)\big|_{B'} = \sqrt{[(2-4\alpha)-2]^2 + 3\cdot[\frac{(-2)-2}{2+2\bar{\nu}}]^2} = 4.19\% \quad \therefore \quad \alpha = 0.844 \tag{5}$$

So, *B'* is located at $(\varepsilon, \gamma) = (2 - 4\alpha, -2) = (-1.378, -2)\%$. The initial point of the count of the second event is *B(–2, 0)*. The relative Mises strains with respect to *B* are given by

$$\varepsilon_{R_{Mises}}(B) = \sqrt{(\varepsilon + 2\%)^2 + 3\cdot[(\gamma - 0\%)/(2+2\bar{\nu})]^2} \tag{6}$$

resulting in the relative history from Fig. 3. The count of this second event stops at point *A* which, together with point *E*, has the largest relative ε_{RMises} with respect to *B*, see Fig. 3. The paths *C-C'* and *E-A* in the γ-ε diagram are arcs of ellipses centered at *B*. Note that it is important to draw the path *B'-F* in these two figures, to avoid counting it more than once. Note also that, if P_i is the initial point of the count, the successive plots $\varepsilon_{RMises}(P_i) \times$*(remaining events)* follow the rules of the traditional rainflow algorithm.

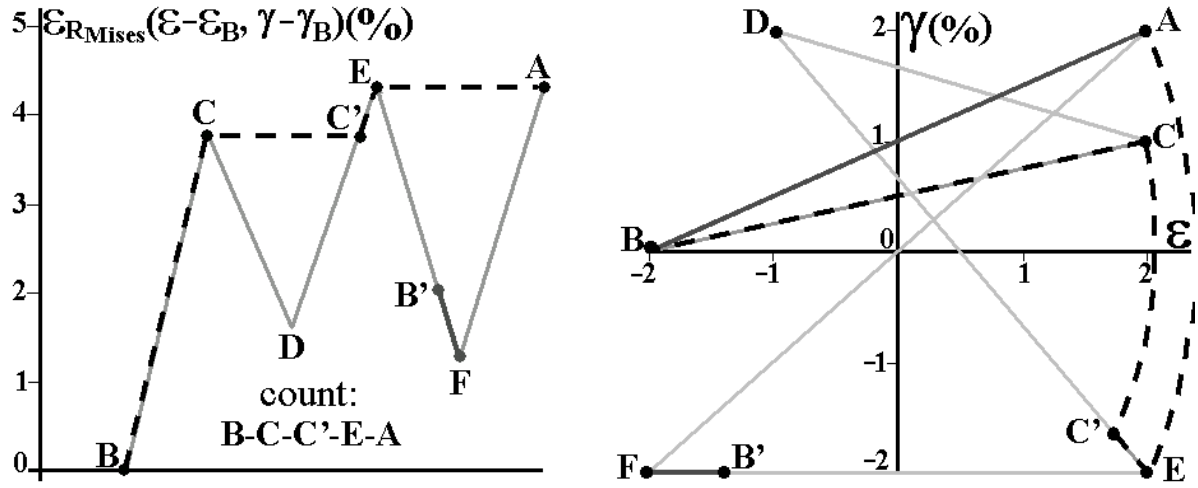

Fig. 3: Rainflow count of the 2nd event of the history and corresponding γ-ε diagram.

The position of point *C'* in the *D-E* path of the γ-ε diagram is interpolated by the expression $(\varepsilon, \gamma) = (-1, 2) + \alpha \cdot [(2, -2) - (-1, 2)]$, where α is the value that makes the ε_{RMises} of *C'* with respect to *B* equal to *4.05%* (which is equal to the ε_{RMises} of *C* with respect to *B*), hence

$$\varepsilon_{R_{Mises}}(B)\big|_{C'} = \sqrt{[(-1+3\alpha)-(-2)]^2 + 3\cdot[\frac{(2-4\alpha)-0}{2+2\bar{\nu}}]^2} = 4.05\% \quad \therefore \quad \alpha = 0.961 \tag{7}$$

So, *C'* is located at $(\varepsilon, \gamma) = (-1 + 3\alpha, 2 - 4\alpha) = (1.883, -1.844)\%$. Along the entire path *B-C-C'-E-A*, the largest value of ε would be higher than *2%*, taking place in the middle of the elliptic arc *E-A* of Fig. 3. Note, however, that the path *E-A* is a result of the rainflow count, it is not an actual path followed during the history. Therefore, it is reasonable to assume that the

largest value of ε is *2%*, which happens exactly at points *E* and *A*. The minimum $\varepsilon = -2\%$ takes place in *B*, resulting in $\Delta\varepsilon = 4\%$ in this count according to Wang-Brown's method. The highest $\gamma = 2\%$ takes place at *A* and the lowest $\gamma = -2\%$ at *E*, resulting in $\Delta\gamma = 4\%$. Be careful not to calculate $\Delta\gamma$ as the difference *(2% – 0%)* between the values of γ at *A* and *B*, the final and initial points of the path, because in this case the lowest value of γ takes place along the path, at point *E*.
A criticism to this procedure that obtains $\Delta\gamma = 4\%$ instead of *2%* is that most of the variation $\Delta\varepsilon$ takes place in the path *B-C'*, whereas most of the variation $\Delta\gamma$ takes place subsequently, in the path *C'-C-E-A*. However, when calculating the associated damage, Wang-Brown's method assumes that both variations take place at the same time, and not sequentially. This could possibly result in conservative predictions in this case. If, on the other hand, only the extremes *A* and *B* of the path were used to calculate the strain variations, obtaining $\Delta\gamma = 2\%$ instead of *4%*, highly non-conservative predictions would be probably obtained. Such inconsistencies will be solved in the Modified Wang-Brown count proposed in the next section, where the MOI method will be used to calculate the equivalent strain (or stress) ranges associated with a complex path.

The third event begins at point *C*, and stops at *B'* because it found a previous count, resulting in the path *C-D-D'-B'*. In the corresponding γ-ε diagram, the transition *D-D'* happens through an arc of ellipse centered at *C*, where the ε_{RMises} relative to *C* is

$$\varepsilon_{R_{Mises}}(C) = \sqrt{(\varepsilon - 2\%)^2 + 3 \cdot [(\gamma - 1\%)/(2 + 2\bar{\nu})]^2} \tag{8}$$

The position of *D'* in the path *E-F* is interpolated by $(\varepsilon, \gamma) = (2, -2) + \alpha \cdot [(-2, -2) - (2, -2)]$, where α makes ε_{RMises} with respect to *C* equal to *3.06%* (the same value as ε_{RMises} of *D* with respect to *C*), hence

$$\varepsilon_{R_{Mises}}(C)\big|_{D'} = \sqrt{[(2 - 4\alpha) - 2]^2 + 3 \cdot [\frac{(-2) - 1}{2 + 2\bar{\nu}}]^2} = 3.06\% \quad \therefore \quad \alpha = 0.609 \tag{9}$$

So, *D'* is located at $(\varepsilon, \gamma) = (2 - 4\alpha, -2) = (-0.437, -2)\%$. Note that along the path *C-D-D'-B'* the largest $\Delta\varepsilon$ takes place between *B'* and *C*, giving a normal strain range $\Delta\varepsilon = 2\% - (-1.378\%) = 3.378\%$, whereas the largest shear strain range $\Delta\gamma$ takes place between the path *D'-B'* and point *D*, with $\Delta\gamma = 2\% - (-2\%) = 4\%$.

The counting procedure for the remaining half cycles of the block is similar, resulting in the half cycles *D-C'*, with normal and shear strain ranges $\Delta\varepsilon = 1.883\% - (-1\%) = 2.883\%$ and $\Delta\gamma = 2\% - (-1.844\%) = 3.844\%$; *E-D',* with $\Delta\varepsilon = 2\% - (-0.437\%) = 2.437\%$ and $\Delta\gamma = 0\%$; and *F-A,* with $\Delta\varepsilon = 4\%$ and $\Delta\gamma = 4\%$, according to Wang-Brown's algorithm.

The multiaxial rainflow count results in the ranges and mean loads shown in Fig. 4, corresponding to the paths *A-B-B'-F*, *B-C-C'-E-A*, *C-D-D'-B'*, *D-C'*, *E-D'* and *F-A*, represented by arrows in the γ-ε diagram.

Multiaxial damage models based on strains, e.g. Brown-Miller, Fatemi-Socie or SWT, can then be applied to these half cycles. Note that the Sines and Findley models are not applicable

in this case, because ε_a and/or $\gamma_a \geq 2\%$ implies in significant plasticity for metals, while those models assume linear elastic strains; besides, Sines' model does not account for NP histories.

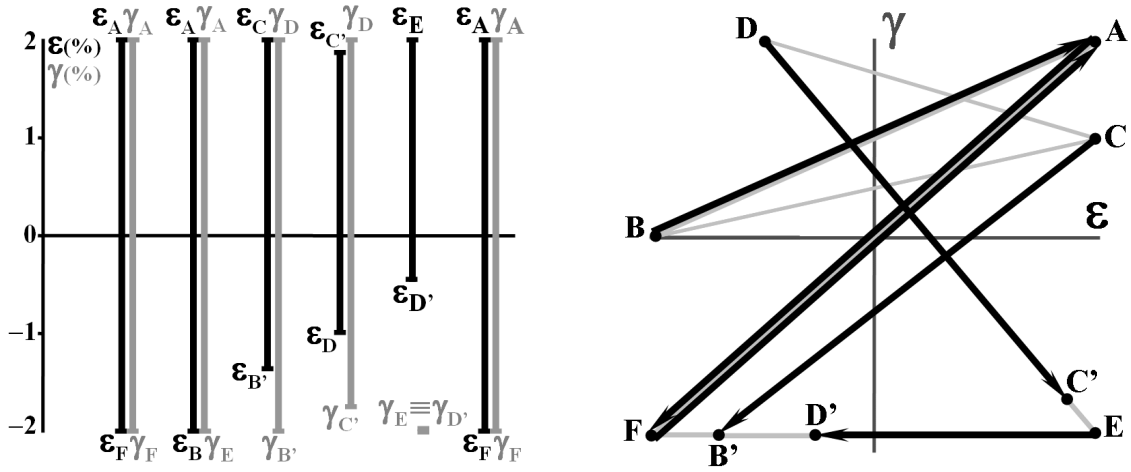

Fig. 4: Rainflow counted strain ranges and corresponding γ-ε diagram with arrows representing the resulting half cycles.

4. MODIFIED WANG-BROWN (MWB) ALGORITHM

The original Wang-Brown algorithm is not difficult to be implemented in histories of uniaxial tension/bending combined with torsion, which can be represented only by one normal σ_x and one shear τ_{xy} stress components (or one normal ε_x and one shear γ_{xy} strain components). In this case, the subspace of normal and shear components is planar (it is represented by a diagram in only 2 dimensions), and the only difficulty in applying the algorithm happens when solving for the equations of the ellipses associated with the points with same relative Mises stress or strain.

However, in a generic multiaxial history, the dimension of the diagram may be increased, requiring the calculation of intersections between straight lines and ellipsoid or hyper-ellipsoid surfaces, increasing the computational complexity.

The Modified Wang-Brown method solves this problem by working in the reduced 5-dimensional stress $E_{5\sigma}$ [3] or strain $E_{5\varepsilon}$ subspaces, or in a lower dimension subspace from them. In this way, a general multiaxial strain or stress history is represented by a set of points $P_i = (e_1, e_2, e_3, e_4, e_5)$ or $P_i = (S_1, S_2, S_3, S_4, S_5)$, respectively, where

$$S_1 \equiv \sigma_x - \frac{\sigma_y}{2} - \frac{\sigma_z}{2} = \frac{3}{2} S_x, \quad S_2 \equiv \frac{\sigma_y - \sigma_z}{2}\sqrt{3} = \frac{S_y - S_z}{2}\sqrt{3}$$
$$S_3 \equiv \tau_{xy}\sqrt{3}, \quad S_4 \equiv \tau_{xz}\sqrt{3}, \quad S_5 \equiv \tau_{yz}\sqrt{3} \tag{10}$$

$$e_1 \equiv \frac{3}{2}\cdot\frac{e_x}{1+\bar{\nu}} = \frac{2\varepsilon_x - \varepsilon_y - \varepsilon_z}{2\cdot(1+\bar{\nu})}, \quad e_2 \equiv \frac{e_y - e_z}{2\cdot(1+\bar{\nu})}\sqrt{3} = \frac{\varepsilon_y - \varepsilon_z}{2\cdot(1+\bar{\nu})}\sqrt{3},$$
$$e_3 \equiv \frac{\gamma_{xy}\sqrt{3}}{2\cdot(1+\bar{\nu})}, \quad e_4 \equiv \frac{\gamma_{xz}\sqrt{3}}{2\cdot(1+\bar{\nu})}, \quad e_5 \equiv \frac{\gamma_{yz}\sqrt{3}}{2\cdot(1+\bar{\nu})} \tag{11}$$

Wang-Brown's multiaxial rainflow algorithm is rather simplified when working in such spaces, because the distance between two points is already the relative Mises strain (or stress) between them. The 3 rules of the rainflow count have now simple geometric interpretations, resulting in:

1. The count must be initiated at the point with highest norm, i.e., with the longest Euclidean distance to the origin of the diagram. This first initial counting point is called P_1, and the subsequent ones are called P_2..., P_n, in the same sequence of the original history.
2. Each count must be sequentially initiated at each point P_i of the diagram.
3. The final point of each counting is obtained when reaching:
   a) the point P_j most distant from the initial point P_i (with $j > i$) in the reduced subspace, or
   b) any path used in a previous count.

The first rule in Wang-Brown's algorithm was conceived to try to guarantee that the largest ε_{RMises} (or relative Mises stress σ_{RMises}) of the history is identified, one of the main objectives of a rainflow count. However, this rule can fail to reach this objective if the point P_1 with largest norm is not one of two points of the diagram farthest apart from each other.

This is easy to check in the example from Fig. 5, which shows an e_1-e_3 strain diagram with a triangular path. The point $(e_1, e_3) = (0.8\%, 0\%)$ is clearly the one with largest norm, equal to 0.8%, however its Wang-Brown count results in two half cycles with $\varepsilon_{RMises} = 1.0\%$. Instead, if the count is started at the point $(e_1, e_3) = (0\%, 0.6\%)$, both half cycles result in $\varepsilon_{RMises} = 1.1\%$. It is not difficult to prove that the largest relative Mises strain (or stress) of the history can be ***underestimated*** by up to $1-\sqrt{2}/2 = 29.3\%$ using the original Wang-Brown algorithm. Even if a convex hull method or the MOI method are applied to the resulting half cycles, to account for the shape of the entire path, and not only the value of ε_{RMises}, the original Wang-Brown algorithm still underestimates the resulting equivalent ranges. The conclusion is that the starting point of the first count must be better chosen.

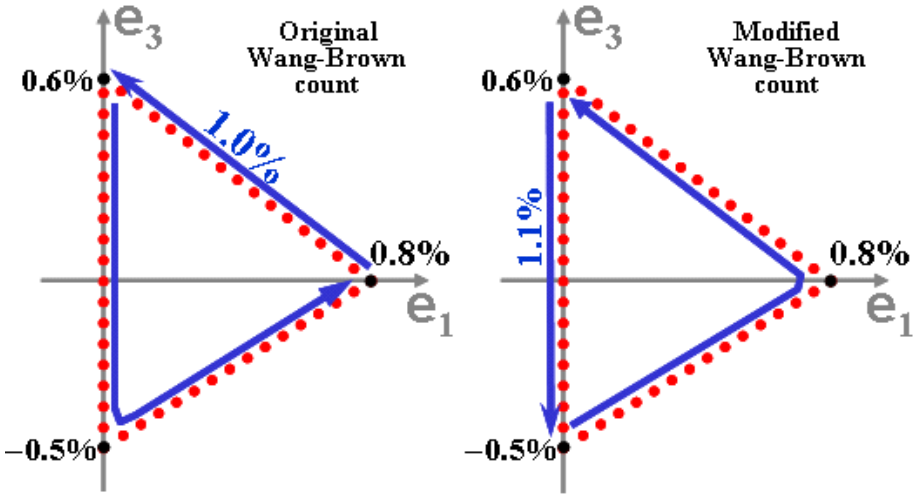

Fig. 5: Rainflow counts using the original Wang-Brown algorithm (left) and the modified version (right).

So, the first rule of the multiaxial rainflow count is now modified, to search for the pair of points in the diagram with largest relative distance, and between them the point P_1 farthest from the origin. But the Modified Wang-Brown (MWB) algorithm differs from the original

method not only due to such first rule. Other rules are modified and introduced as well. The MWB method can be summarized by a set of 8 rules:

1. Find among the $n \cdot (n-1)/2$ pairs of points from an n-point path the one(s) that form the longest chord in the 5D strain (or stress) subspace, and choose among them the one with greatest distance from the origin; label this point P_1, and the subsequent P_2, ..., P_n following their original order;
2. Each count should be sequentially initiated at P_1, P_2, ..., P_i, ..., P_n;
3. The final point in each count is obtained when reaching:
   a) the point P_j farthest away (in an Euclidian sense) from the initial point P_i ($j > i$), or
   b) any finite segment (not just a point or a finite number of points) from a previous count;
4. Once found the initial and final points P_i and P_j, the count is defined by the traveled path portions closest to the straight segment P_i-P_j in an Euclidean sense (to avoid long "detours" from the straight line P_i-P_j that defines such half cycle);
5. Every time a full cycle is counted, i.e. two half cycles with identical extreme points are counted, use the Moment Of Inertia (MOI) method (or some convex hull method) to calculate the equivalent strain (or stress) range or amplitude and mean or maximum from the full cycle to obtain the associated fatigue damage using some multiaxial model;
6. After rainflow counting the entire load history, repeat step 5 to calculate the damage contribution of the half cycles that did not close into a full cycle;
7. Use some damage accumulation rule, e.g., Miner's rule, to find the total multiaxial damage;
8. If using a critical plane approach, repeat steps 1-7 for every candidate plane, to find the critical plane that maximizes the accumulated multiaxial damage; note that only Case B cracks or tension-torsion histories will need a multiaxial rainflow count, because the single shear component in Case A cracks can be counted using a uniaxial rainflow algorithm.

5. APPLICATION OF THE MWB ALGORITHM

In this section, the MWB rainflow algorithm is applied to the NP history presented in Section 3, formed by blocks of $(\varepsilon_x, \gamma_{xy}) = \{(2, 1) \rightarrow (-1, 2) \rightarrow (2, -2) \rightarrow (-2, -2) \rightarrow (2, 2) \rightarrow (-2, 0)\}\%$ repeatedly applied to a steel specimen. The MWB count results in this example in the exact same half cycles from the original Wang-Brown method obtained in the example from Section 3, however with a much lower complexity and computational cost. The MWB algorithm has simple geometric interpretations, it does not require the calculation of intersections with hyperellipses, and it does not require the recalculation of all ε_{RMises} for every count. In addition, it always finds the events with largest ε_{RMises}, as opposed to the traditional Wang-Brown method, as discussed before.

After obtaining the equivalent ranges and mean components of all rainflow counted paths, any multiaxial model can be applied to calculate the accumulated damage at the considered candidate plane. The critical plane will then be the candidate plane with highest accumulated damage.

6. CONCLUSIONS

Wang and Brown proposed a multiaxial rainflow count based on the relative Mises strain ε_{RMises} as an indirect measure of the damage during a half cycle. But the original method requires the calculation of ε_{RMises} at every rainflow count for all subsequent starting points. In this work, a Modified Wang Brown (MWB) rainflow counting method was proposed, based on the representation of the stress or strain history in a reduced 5D subspace of the 6 deviatoric strain (or stress) components. The MWB uses improved rules to guarantee that the event

with highest ε_{RMises} is always counted. Coupled with some convex hull method, the MWB can better account for the path shape influence on the associated fatigue damage. The method has simple geometric interpretations that considerably simplify its implementation, e.g. the distance between 2 points in the considered deviatoric strain subspace is the ε_{RMises} between them.

REFERENCES

[1] Socie, D.F., Marquis, G.B. Multiaxial Fatigue, SAE 1999.

[2] Wang, C.H., Brown, M.W., Life prediction techniques for variable amplitude multiaxial fatigue - part 1: theories. Journal of Engineering Materials and Technology 118, pp.367-370, 1996.

[3] Papadopoulos, I.V., Davoli, P., Gorla, C., Fillippini, M., Bernasconi, A., A comparative study of multiaxial high-cycle fatigue criteria for metals. International Journal of Fatigue 19(3), pp.219–235, 1997.

[4] Matsuishi, M., Endo, T., Fatigue of metals subjected to varying stresses, Japan Society of Mechanical Engineers, 1968.

[5] ASTM E 1049, Practices for cycle counting in fatigue analysis, ASTM Standards v.03.02.

[6] Meggiolaro, M.A., Castro, J.T.P., ViDa - Programa para Previsão de Vida à Fadiga sob Carregamentos Complexos, III Simpósio de Análise Experimental de Tensões, pp.7-10, PUC-Rio, Brazilian Society of Mechanical Sciences and Engineering, 1995 (in Portuguese).

[7] Miranda, A.C.O., Meggiolaro, M.A., Castro, J.T.P., Martha, L.F., Bittencourt, T.N., Fatigue Crack Propagation under Complex Loading in Arbitrary 2D Geometries, Applications of Automation Technology in Fatigue and Fracture Testing and Analysis: 4th Volume, ASTM STP 1411, American Society for Testing and Materials, West Conshohocken, PA, USA, pp.120-145, 2002.

[8] Miner, M.A., Cumulative damage in fatigue, Journal of Applied Mechanics v.12, pp.A159-A164, 1945.

[9] Bannantine, J.A., Socie, D.F., A Variable amplitude Multiaxial Fatigue Life Prediction Method, fatigue Under Biaxial and Multiaxial Loading, ESIS Publication 10, Mechanical Engineering Publications, London, pp.35-51, 1991.

[10] Wang, C.H., Brown, M.W., Life prediction techniques for variable amplitude multiaxial fatigue - part 1: theories, Journal of Engineering Materials and Technology, v.118, pp.367-370, 1996.